

# VICI Yearly report 2013

D. Krijgsman

March 18, 2013

**Title of the project** Bridging the gap between particulate systems and continuum theory

## **Project aim**

The gap between discrete (micro) and continuum (macro) concepts for the modelling and understanding of particulate systems is bridged by micro-macro transition methods. Modern discrete particle-based models describe the particles in detail, but are of limited value for studying industrial processes and natural phenomena since too many particles are involved. Continuum methods, on the other hand, are readily applied in engineering applications. However, continuum methods rely on empirical constitutive laws with phenomenological parameters that disregard both the discrete nature of particles and the micro-structure. Micro-macro transition methods are being developed to combine the advantages of discrete and continuum models.

## **Progress**

A novel local constitutive model based on observations from discrete element simulations has been developed for small-scale deformations of a quasi steady bi-axial geometry. The model consists of non-linear evolution equations for both shear stress and anisotropy, where the anisotropy is used to model the history dependence of the material. The main advantage of the model is that it only consists of 5 material parameters, where comparable constitutive usually require many more. Several discrete particle simulations were performed to test the model's accuracy for various deformation modes. In the attached paper this has been done for small cyclic pure shear, where it has been shown that the model is able qualitatively model the transient as well as the limit cycles. Future work will include extending the model to generic three-dimensional cases and implementing it in a finite element method. The objective is to predict stresses and strains in macro scale applications, taking into account the evolution of the microscopic material structure.

# 2D cyclic pure shear of granular materials, DPM and model

D. Krijgsman and S. Luding

*Multi Scale Mechanics, Universiteit Twente, Faculty of Engineering Technology, MESA+,  
P.O. Box 217, 7500 AE Enschede, The Netherlands*

**Abstract.** DPM simulations of granular materials under 2D, isochoric, cyclic pure shear have been performed and are compared to a recently developed constitutive model involving a yield stress, dilatant stresses and structural anisotropy. The original model shows the cyclic response qualitatively, but suffers from an artificial drift of pressure. With a small modification in the definition of the stress anisotropy and an additional limit-pressure term in the evolution equation for the pressure, it is able to show the transient stage as well as the limit cycles. The overall goal – beyond the scope of the present study – is to develop a local constitutive model that is able to predict real life, large scale granular systems.

**Keywords:** Granular, Pure Shear, DPM, Constitutive model, Anisotropy  
**PACS:** 45.70, 81.05.Rm, 83.30.Fg

## INTRODUCTION

Dense granular materials are widely encountered in industrial processes, such as hopper discharge, chute flow and fluidized beds. Grains in these materials interact with multiple neighbours for finite durations and stress is largely transmitted through force chains. Due to the disordered behaviour of these particles, the materials show peculiar mechanical properties quite different from classical fluids or solids, like dilatancy, yield stress, history dependence and anisotropy. The DPM method, in which the forces on each particle are calculated and integrated over a finite time, is able to capture all of these properties, however has the major drawback that it is computationally too expensive for realistic, large scale systems.

Constitutive models are an option to simulate real problems instead of just laboratory scale experiments with widely available methods like FEM or CFD. Many of such models have been developed in literature [1, 2, 3, 4], which all have their own advantages and disadvantages. In this work a further look is given to the model proposed and applied to cycling loading by Magnanimo and Luding [5, 6]. Besides equations for the stresses, the model also incorporates an evolution equation for the anisotropy, which allows it to predict dilatancy, cope with the history dependent nature of the material, and provide anisotropic material properties, including a yield stress.

Simulations are performed by the DPM package Mercury [7] and used to calibrated to the model, both to the original and the modified version.

## CONSTITUTIVE MODEL

In this section a short overview of the used constitutive model is given. For more information the reader is re-

ferred to the original work [5, 6]. The local model starts from the incremental Hooke's Law:

$$\delta\sigma_{ij} = C_{ijkl}\delta\varepsilon_{kl} \quad (1)$$

From there it assumes that in the bi-axial box system, the stress and strain tensors only have diagonal components, such that they can be split into volumetric and deviatoric parts, leading to:

$$\begin{bmatrix} \delta\sigma^h \\ \delta\tau \end{bmatrix} = \begin{bmatrix} 2B & A \\ A & 2G \end{bmatrix} \begin{bmatrix} \delta\varepsilon^v \\ \delta\gamma \end{bmatrix} \quad (2)$$

now it is the goal to find expressions for the bulk modulus  $B$ , the shear modulus  $G$  and the anisotropy modulus  $A$ . Two modifications of the elastic model with constant moduli are in, a non-linear stress evolution (with yield stress) and a varying anisotropy, while initially  $B$  and  $G$  are assumed constant. In this paper a third additional modification is proposed called the pressure stabilization.

### Non-linear stress evolution

From DEM simulations it has been widely observed that for increasing shear strains, the stress increments decrease until the stress saturates in the critical state regime. This is modelled by multiplying the incremental shear strain with the stress anisotropy  $S$ :

$$\begin{bmatrix} \delta\sigma^h \\ \delta\tau \end{bmatrix} = \begin{bmatrix} 2B & A \\ A & 2G \end{bmatrix} \begin{bmatrix} \delta\varepsilon^v \\ S\delta\gamma \end{bmatrix} \quad (3)$$

with

$$S = 1 - \frac{\tau}{\sigma^h} \frac{\text{sign}(\delta\gamma)}{s_{max}^d} \quad (4)$$

where  $s_{max}^d = \left(\frac{\tau}{\sigma^h}\right)_{max}$  is the absolute maximum allowable deviatoric stress ratio in the material after long shear deformation.

### Varying anisotropy

The second modification is to prescribe the anisotropy modulus as an evolution equation dependent on the shear strain:

$$\frac{dA}{d\gamma} = \beta_A (A_{max} - \text{sign}(\delta\gamma)A) \quad (5)$$

with  $A_{max}$  the absolute maximum allowable anisotropy in the material and  $\beta_A$  a parameter that determines how fast the anisotropy changes and thus how fast saturation is approached. If  $\delta\gamma$  does not change sign, equation (5) can be solved analytically:

$$A = \text{sign}(\delta\gamma)A_{max} \left(1 - e^{-\beta_A|\gamma|}\right) + e^{-\beta_A|\gamma|}A_0 \quad (6)$$

with  $A_0$  the initial anisotropy at  $\gamma = 0$ .

### Pressure stabilization

On top of these two features a new pressure stabilization term is proposed. The goal of this term is to stabilize the model for shear cycles (otherwise the pressure would continuously in/decrease), as well as to provide a better model for the initial transient stage leading to the limit cycles. The term is a simple addition to the differential pressure equation in the form of:

$$\beta_p \left( \sigma_{steady}^h(\phi) - \sigma^h \right) |\delta\gamma| \quad (7)$$

where  $\beta_p$  is a rate parameter and  $\sigma_{steady}^h(\phi)$  is the expected steady state pressure dependent on the packing fraction. In this paper, however, only one packing fraction is studied, so the dependence on the packing fraction is omitted throughout this paper.

## SIMULATIONS

The results from the model are compared with DPM simulation. These simulations are performed by the DPM package Mercury [7], which integrates Newtons equations of motion for a large number of particles a velocity Verlet algorithm. The forces are due to interaction between particles (modelled as a visco-elastic normal force) and a much smaller background friction:

$$m\ddot{\vec{x}}_i = \vec{f}_i = \gamma_b \dot{\vec{x}}_i + \sum_{i \neq j} \left( k\delta_{ij} + \gamma_p \dot{\delta}_{ij} \right) \vec{n}_{ij} \quad (8)$$

where  $\gamma_b$  is the background friction,  $\vec{x}_i$  the location of particle  $i$ ,  $k$  the contact stiffness,  $\delta_{ij}$  the overlap between particles  $i$  and  $j$ ,  $\gamma_p$  the inter particle viscosity and  $\vec{n}_{ij}$  the normal vector pointing from particle  $j$  to  $i$ . The parameters used in this study are shown in table 1. To remove the effect of walls on the simulation, both boundaries are modelled as periodic walls.

**TABLE 1.** Simulation parameters

Parameter	Value	Explanation
$k$	10000 Nm <sup>-1</sup>	Contact stiffness
$\gamma_p$	0.2938 Nsm <sup>-1</sup>	Inter particle viscosity
$\gamma_b$	0.0294 Nsm <sup>-1</sup>	Background friction
$\rho$	20 kgm <sup>-3</sup>	Particle density
$\Delta t$	1.3 · 10 <sup>-5</sup> s	Simulation time step
$t_c$	6.5 – 13 · 10 <sup>-4</sup> s	Collision time
$r_n$	0.80 – 0.89	Coefficient of restitution

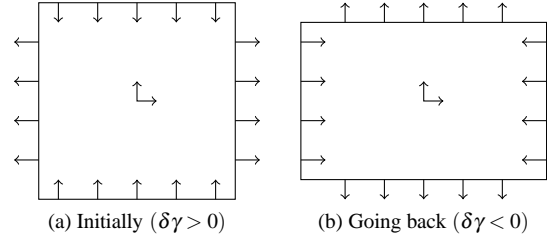


**FIGURE 1.** Deformation mode

### Initial conditions

The initial packing is prepared by inserting 10 000 particles with a homogeneous size distribution ( $r^{min} = 3.7 \cdot 10^{-3}$  m and  $r^{max} = 7.4 \cdot 10^{-3}$  m) at random positions (with small random velocities) in a large square initial domain. Then the system is slowly compressed to the desired packing fraction,  $\phi = 0.85$ , where it equilibrates until the kinetic energy has decayed to very small values.

### Simulation details

During the simulation the particles are subjected to pure shear cycles (see figure 1). Pure shear is induced by moving the two periodic walls while conserving the volume. The walls move slowly according to a sinus (half) profile, until a maximum shear strain of  $\gamma = 0.001$ . After it has reached its maximum strain amplitude, the shear direction is reversed and the simulation continues until the original shape of the box is retained at the end of each cycle. One complete cycle takes  $4 \cdot 10^6$  time steps and the ratio of kinetic to potential energy is always small ( $E_k/E_p < 0.002$ ). Therefore, it is assumed that the systems is in the quasi-static, shear rate independent regime. Note that, even though size and shape of the box, at the start and at the end, are the same, the stress and anisotropy states change dramatically.

## RESULTS

In the DPM simulations an initial transient stage is clearly visible until after about 100 cycles. From there

on the system is in a state where limit cycles are present (see the pressure variation in figure 3). First the limit cycles are discussed and later the transient stage.

### Limit cycles

The evolution of the pressure and the shear stress over pressure ratio, during a shear cycle in the limit cycle state, are shown in figure 2. Here the stress curves form closed loops, meaning that the stress state at the start and at the end of a cycle are equal. At the start of each cycle more of the contacts between particles will be aligned in the compressive direction of the previous half-cycle, giving rise to the structural anisotropy and the corresponding anisotropy modulus  $A$  (data not shown). At each strain reversal, the contacts in the previously dominant direction will become weaker or even open, resulting in a drop of anisotropy and pressure and an increase in shear stress. As the simulation continues, the smaller fraction of contacts in the shear compression direction will become stronger and new contacts can form. Halfway trough the first half of the cycle, loosening and strengthening of contacts are in equilibrium, resulting in a roughly constant pressure, whereas the shear stress continues to increase. Near the end of first half-cycle, the slope of the shear stress curve starts to decrease, meaning that the system is starting to saturate. If one would continue to shear in the same direction, finally the pressure would also saturate. In the second half-cycle the system will experience a similar opening and closing of contacts, but with exchanged directions, until it returns to its initial state.

To fit the simulation data of a single cycle with the model, it has been numerically integrated over the shear cycle and at 80 points compared to the simulations, resulting in an error. A weighted non-linear least squares fitting procedure is used to reduce the error and obtain an optimal fit.

The model is qualitatively able to reproduce the simulations. All of the three phases discussed before show the correct behaviour. However, two distinct differences are visible: First, the locations of the minima in the pressure; In the simulations the minimum of pressure is almost in the symmetry (centre) point, whereas the model shows two minima, closer to the shear reversals. Secondly, the model suffers from a tiny but significant drift in pressure. To be able to produce limit cycles (i.e. the variables having the same value at the start end at the end of each cycle) the model has to be symmetric around the average deformation, which is achieved by the correction term in equation (7).

### Isotropic stress saturation

The need for an additional term also shows up if one does not only look at the last (stable) cycles, but also on the approach to this state. In figure 3 the evolution of the pressure is shown as a function of the number of cycles

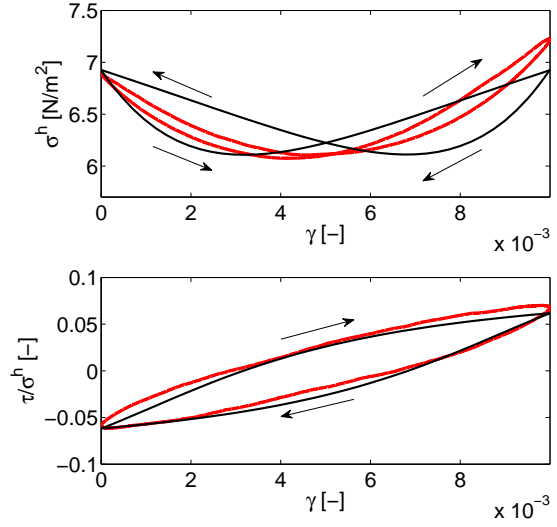


**FIGURE 2.** Evolution of pressure, and the shear stress over pressure ratio during a cycle after 200 cycles. Arrows indicate the direction of shear; for a more clear picture averages are taken over the last 50 cycles. Black lines are averages of the simulation results and the red lines are a fit using the model (both the improved as the original model show the same behaviour)

for 4 different simulations. Due to the isotropic preparation phase the initial packings have a high pressure. During the shear cycles the particles wiggle around and find more efficient packings, resulting into less overlap and a significantly reduced pressure. As more cycles are simulated the pressure at the start of each cycle saturates at roughly  $6.5 \text{ Nm}^{-2}$ .

To search for the instability of the model and to be able to obtain stable limit cycles, the model is analytically examined in the limit of small pressure variations around an average pressure (note that this is not the case in the simulation results). In this limiting case the same pressure is used as in the pressure stabilization term ( $\sigma_{steady}^h$ ), so that equation (4) simplifies to:

$$S = 1 - \frac{\tau}{\sigma_{steady}^h} \frac{\text{sign}(\delta\gamma)}{s_{max}^d} \quad (9)$$

which makes the whole set of equations analytically solvable, resulting in:

$$\sigma^h = C_1 + A_{max} \left( \frac{4}{\xi + \beta_A} e^{-(\xi + \beta_A)\gamma} - \frac{2}{\xi} e^{-\xi\gamma} \right) \quad (10)$$

$$\tau = \sigma_0^h s_{max}^d \left( 1 - C_2 e^{-\gamma\xi} \right) \quad (11)$$

with  $\xi = 2G/\sigma_{steady}^h s_{max}^d$ . To obtain limit cycles the pressure at the start and the end of the cycle have to be equal,

**TABLE 2.** Parameter values used for the fit with the two model versions and three initial conditions. The original model predicts the behaviour only in the limit cycle regime and requires other initial conditions. The initial conditions of the improved model are the same as used in the simulations, starting from an isotropic initial state.

Parameter	Original Model	Improved model	Explanation
$G$	$5 - 0.2 \text{ Nm}^{-2}$	$5 - 0.2 \text{ Nm}^{-2}$	Shear modulus
$s_{max}^d$	0.097	0.097	Maximal deviatoric stress ratio
$A_{max}$	$593 \text{ Nm}^{-2}$	$593 \text{ Nm}^{-2}$	Maximum anisotropy
$\beta_A$	159	n.a.	Anisotropy growth factor
$\beta_P$	n.a.	2.5	Pressure growth factor
$\sigma_{steady}^h$	n.a.	$6.3 \text{ Nm}^{-2}$	Steady state pressure
$\sigma_0^h$	$6.93 \text{ Nm}^{-2}$	$25 \text{ Nm}^{-2}$	Initial pressure
$\tau_0$	$-0.227 \text{ Nm}^{-2}$	$0 \text{ Nm}^{-2}$	Initial deviatoric stress
$A_0$	$403 \text{ Nm}^{-2}$	$0 \text{ Nm}^{-2}$	Initial anisotropy

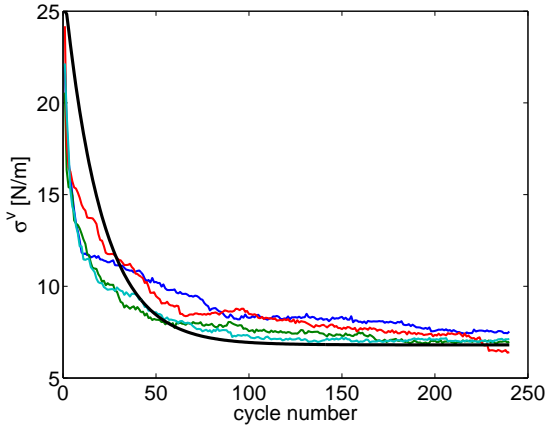


**FIGURE 3.** Evolution of the pressure at the start of each cycle ( $\gamma = 0$ ). Green, blue red and cyan curves show result for 4 different simulations, the black curve shows results of the improved model.

while the shear stress should have changed sign. For simplicity we assume infinite long shear.

$$\begin{aligned} \sigma^h(0) &= \sigma^h(\infty) & \xi &= \beta_A \\ \tau(0) &= -\tau(\infty) & C_2 &= 2 \end{aligned} \quad (12)$$

How to incorporate equations (12) exactly is still an ongoing research, but in this paper  $\beta_A$  has been removed as a free variable. The results of the improved model can be seen in figures 2 and 3.

## CONCLUSION

In this paper DPM simulations of granular materials under 2D, isochoric, cyclic pure shear have been compared to a recently proposed constitutive model. Originally the

model is able to show the limit cycles qualitatively, but was unable to model the transient stage and suffered from a drift in pressure. With a small modification in the definition of the stress anisotropy and an additional term in the evolution equation for the pressure it predicts the transient stage as well as the limit cycles.

Further research will be performed on the influence of the magnitude of the shear strain, the packing fraction and the initial preparation procedure. Present research [8] also suggests that the symmetry of the shear cycles is relevant for the stress state, especially during the first few cycles, an issue to be studied in more detail.

## Acknowledgments

The authors thank the NWO/STW VICI grant 10828 for financial support.

## REFERENCES

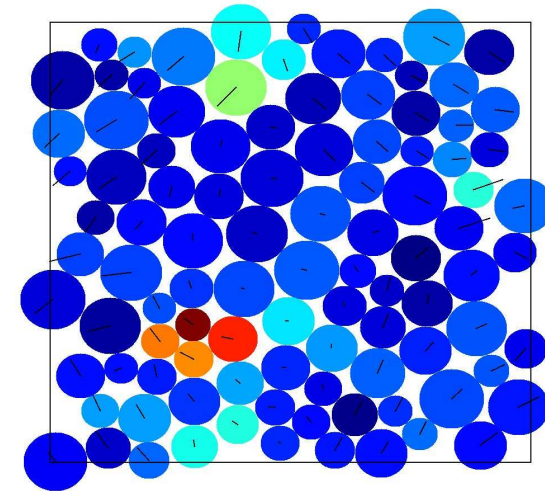
1. J. Sun, and S. Sundaresan, *J. Fluid Mech.* **682**, 590–616 (2011).
2. Y. Jiang, and M. Liu, *Granular Matter* **11**, 139–156 (2008).
3. J. Goddard, *Granular Matter* **12**, 145–150 (2010).
4. I. Einav, *International Journal of Solids and Structures* **49**, 1305–1315 (2012).
5. V. Magnanimo, and S. Luding, *Granular Matter* **8**, 225–232 (2011).
6. S. Luding, and S. Perdahcioglu, *Chemie Ingenieur Technik* **38**, 672–688 (2011).
7. A. Thornton, D. Krijgsman, R. Fransen, S. Gonzalez, D. Tunuguntla, A. Voortwis, S. Luding, O. Bokhove, and T. Weinhart, Mercury-dpm: Hierarchical grid discrete particle simulator (2013).
8. J. Ren, J. Dijkstra, and R. Behringer, Reynolds pressure and relaxation in a sheared granular system (2013), <http://lanl.arxiv.org/abs/1207.7100>.

## Quasi steady Discrete Particle Method

D. Krijgsman

University of Twente

March 19, 2013



## Simulations details

- ▶ Cyclic pure shear (max shear is  $\gamma_{max} = 1\%$ )
- ▶ 2D soft cylinders ( $10^4$  Particles)
- ▶ Polydisperse ( $r_{large} = 2r_{small}$ , uniform size distribution)
- ▶ Bi-axial box
- ▶ Periodic walls
- ▶ Linear normal forces and dissipation (data based on small particles)
  - ▶ Collision time ( $t_c = 6.5 \cdot 10^{-4}$  s)
  - ▶ Coefficient of restitution ( $r = 0.8$ )
- ▶ No tangential forces
- ▶ Small background friction ( $\gamma_{bg} = 0.1\gamma_{pp}$ )

## Wall movement

$$x = x_0 \left( 1 + \gamma_{max} \left( 1 - \cos \left( \frac{\pi t}{N_t \Delta t} \right) \right) \right) \quad s \in [0, N_t \Delta t]$$

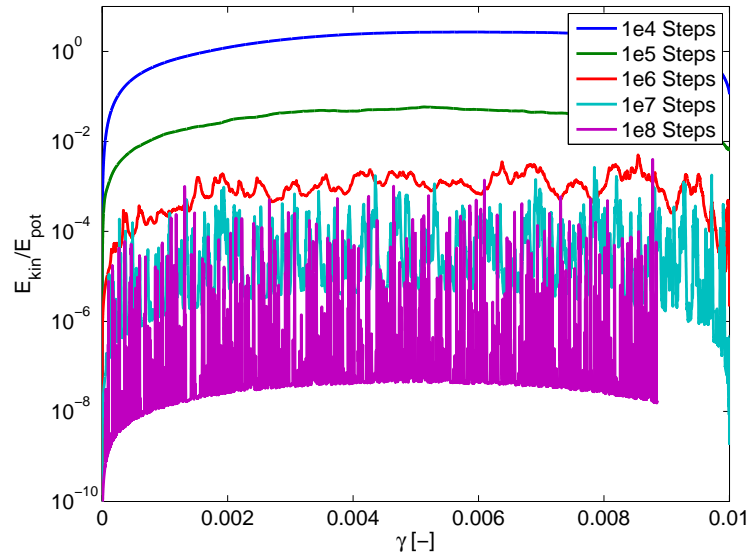
$$\frac{dx}{dt} = \frac{\pi x_0 \gamma_{max}}{N_t \Delta t} \sin \left( \frac{\pi t}{N_t \Delta t} \right)$$

The big question, how large thus  $N$  have to be?  
Inertial number:

$$I = \frac{\dot{\gamma} d}{\sqrt{\frac{P}{\rho}}} = 100 \frac{\gamma_{max}}{N_t} \sqrt{\frac{k}{P\pi}} \leq 10^{-3}$$

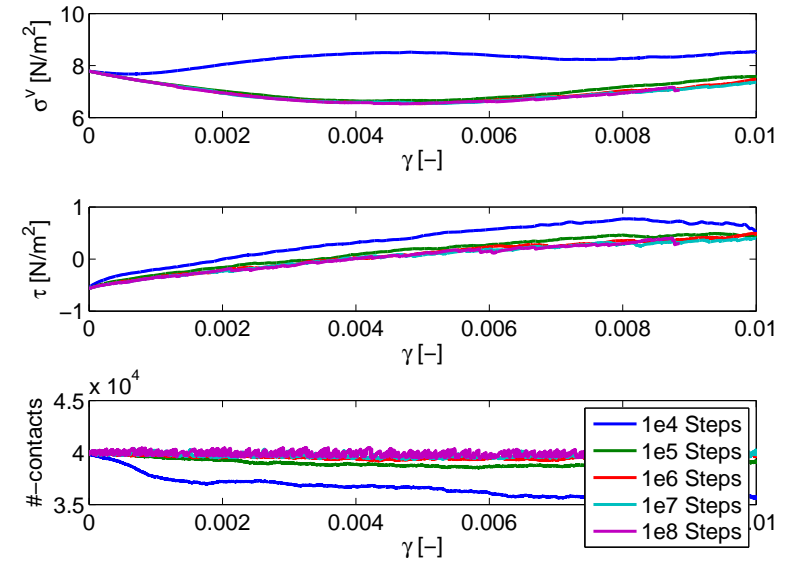
$$N_t \geq 10^5 \gamma_{max} \sqrt{\frac{k}{P\pi}} \approx 20000$$

## Simulation energy ratios



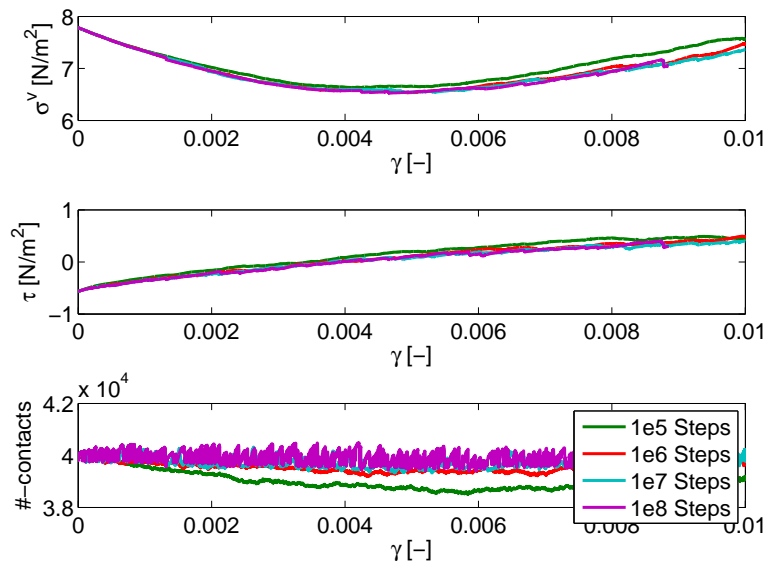
Navigation icons: back, forward, search, etc.

## Simulation stresses



Navigation icons: back, forward, search, etc.

## Simulation stresses



Navigation icons: back, forward, search, etc.

## Computational time

Number of time steps	Computational time
$10^4$	1.8 min
$10^5$	14 min
$10^6$	155 min $\approx$ 2.5 hour
$10^7$	1440 min $\approx$ 1 day
$10^8$	Not yet finished

Navigation icons: back, forward, search, etc.

# DPM

Normal DPM

$$\vec{x}_i = \frac{1}{m_i} \sum_{j \in C_i} k^n \vec{\delta}_{ij} + \gamma^n \vec{\delta}_{ij}$$

Steady state:

$$0 = \frac{1}{m_i} \sum_{j \in C_i} k^n \vec{\delta}_{ij}$$

$N$  coupled non-linear equations, equal to minimising (locally)

$$E_{pot} = \frac{k}{4} \sum_i \sum_{j \in C_i} |\vec{\delta}_{ij}|^2$$



# Quadratic approximation

For small  $\vec{s}$  the potential energy can be approximated as:

$$E_{pot}(\vec{x} + \vec{s}) \approx E_{pot}(\vec{x}) + \vec{x}^t \vec{b} + \frac{1}{2} \vec{s}^t A \vec{s} = f(\vec{s})$$

With  $\vec{b}$  the forces on all the particles and  $A$  the stiffness matrix. Calculating these variables takes a run of the contact detection algorithm.



# Gradient descent minimisation

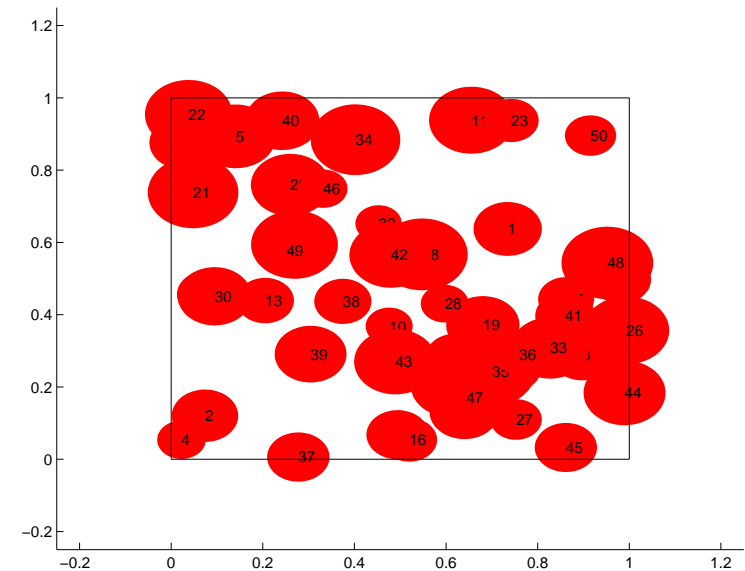
$$E_{pot}(\vec{x} + \vec{s}) \approx E_{pot}(\vec{x}) + \vec{s}^t \vec{b} + \frac{1}{2} \vec{s}^t A \vec{s} = f(\vec{s})$$

- ▶ Choose starting point  $\vec{x}_0$
- ▶ Iterate
  - ▶ Make quadratic approximation  $f(\vec{s})$  of  $E_{pot}(\vec{x} + \vec{s})$
  - ▶ Search direction  $\vec{r}_i = -\vec{\nabla} f(\vec{s}) = -\vec{b} - A\vec{x}$
  - ▶ Pick  $\alpha_i = \frac{\vec{r}_i^t \vec{r}_i}{\vec{r}_i^t A \vec{r}_i}$ , to minimise  $f(\vec{x}_i + \alpha_i \vec{r}_i)$
  - ▶ Search step  $\vec{x}_{i+1} = \vec{x}_i + \alpha_i \vec{r}_i$

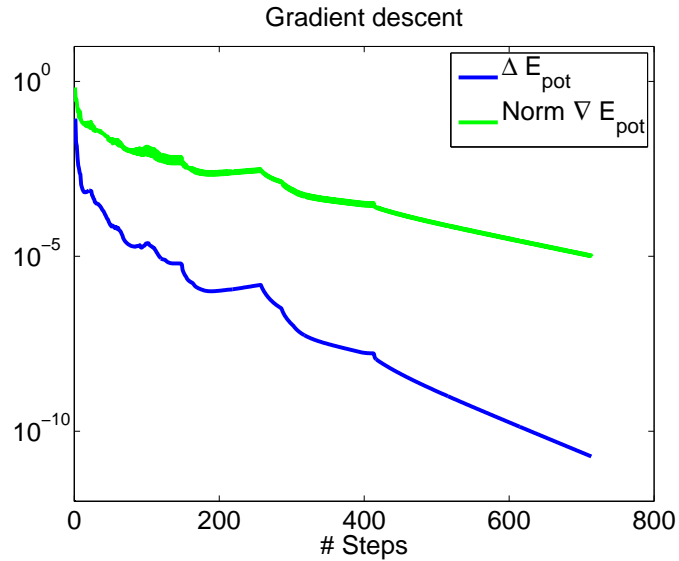
In general convergence rate  $\frac{\kappa(A)-1}{\kappa(A)+1}$



# Gradient descent video



## Gradient descent convergence



## Newton's method

$$E_{pot}(\vec{x} + \vec{s}) \approx E_{pot}(\vec{x}) + \vec{s}^t \vec{b} + \frac{1}{2} \vec{s}^t A \vec{s}$$

Idea, choose  $\vec{r}_i = -A^{-1}\vec{b}$  the exact solution to the quadratic problem, however this leads to problems:

- ▶ How to calculate  $A^{-1}\vec{b}$ ?
- ▶ What if  $A$  is not positive definite?
- ▶ Step size can be so large that approximation no longer holds?

## Trust region method

$$E_{pot}(\vec{x} + \vec{s}) \approx E_{pot}(\vec{x}) + \vec{s}^t \vec{b} + \frac{1}{2} \vec{s}^t A \vec{s}$$

Idea, minimise  $c + \vec{s}^t \vec{b} + \frac{1}{2} \vec{s}^t A \vec{s}$ , subject to  $\|\vec{s}\| \leq \Delta$

## Trust region algorithm

- ▶ Choose starting point  $\vec{x}_0$  and maximum step size  $\Delta_{max}$
- ▶ Set  $\Delta = \Delta_{max}$
- ▶ Iterate
  - ▶ Make quadratic model  $f(\vec{s})$  of  $E_{pot}(\vec{x}_k + \vec{s})$
  - ▶ Solve trust-region subproblem approximately to obtain  $\vec{s}$
  - ▶ Based on  $q_k = \frac{E_{pot}(\vec{x}_k) - E_{pot}(\vec{x}_k + \vec{s})}{E_{pot}(\vec{x}_k) - f(\vec{s})}$ 
    - ▶  $q \geq 0.75$   
Very successful step  
 $\vec{x}_{k+1} = \vec{x}_k + \vec{s}$  and  $\Delta = \min(2\Delta, \Delta_{max})$
    - ▶  $0.25 \leq q < 0.75$   
Successful step  
 $\vec{x}_{k+1} = \vec{x}_k + \vec{s}$
    - ▶  $q < 0.25$   
Unsuccessful step  
 $\vec{x}_{k+1} = \vec{x}_k$  and  $\Delta = \frac{1}{2}\Delta$

## Conjugate gradient

Task: Minimise

$$\vec{s}^t \vec{b} + \frac{1}{2} \vec{s}^t A \vec{s}$$

- ▶ Initialise  $\vec{s}_0 = 0$ ,  $\vec{r}_0 = \vec{b}$  and  $\vec{p}_0 = -\vec{r}$
- ▶ Iterate
  - ▶  $\alpha = \frac{\vec{r}_i^t \vec{r}_i}{\vec{p}_i^t A \vec{p}_i}$  (Obtain step size for quadratic model)
  - ▶  $\vec{s}_{i+1} = \vec{s}_i + \alpha \vec{p}_i$  (Update  $\vec{s}$ )
  - ▶  $\vec{r}_{i+1} = \vec{r}_i + \alpha A \vec{p}_i$  (Equivalent to  $\vec{r}_{i+1} = A \vec{s}_{i+1} + \vec{b}$ )
  - ▶  $\beta = \frac{\vec{r}_{i+1}^t \vec{r}_{i+1}}{\vec{r}_i^t \vec{r}_i}$
  - ▶  $\vec{p}_{i+1} = \beta \vec{p}_i - \vec{r}_i$  (Update search direction)

In general convergence rate  $\frac{\sqrt{\kappa(A)}-1}{\sqrt{\kappa(A)}+1}$



## Trust region subproblem

Task: Solve approximately

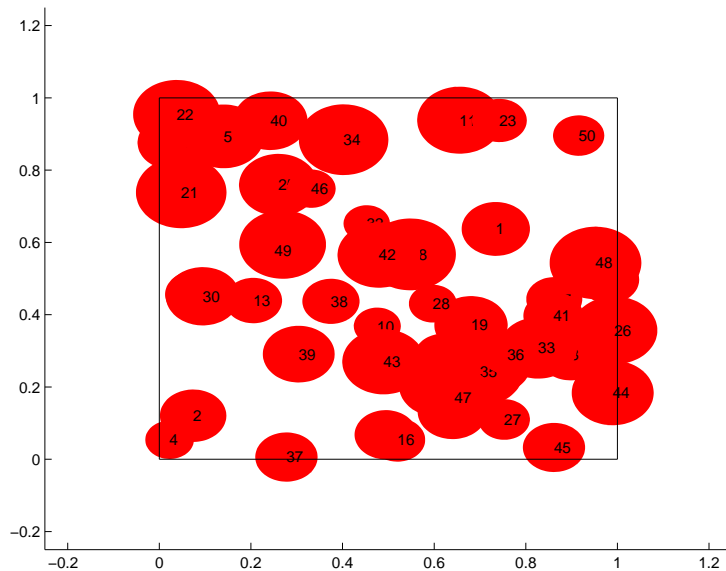
$$\min \left( \vec{s}^t \vec{b} + \frac{1}{2} \vec{s}^t A \vec{s} \right) \quad s.t. \quad \|\vec{s}\| \leq \Delta$$

Solution: Perform conjugate gradient steps until

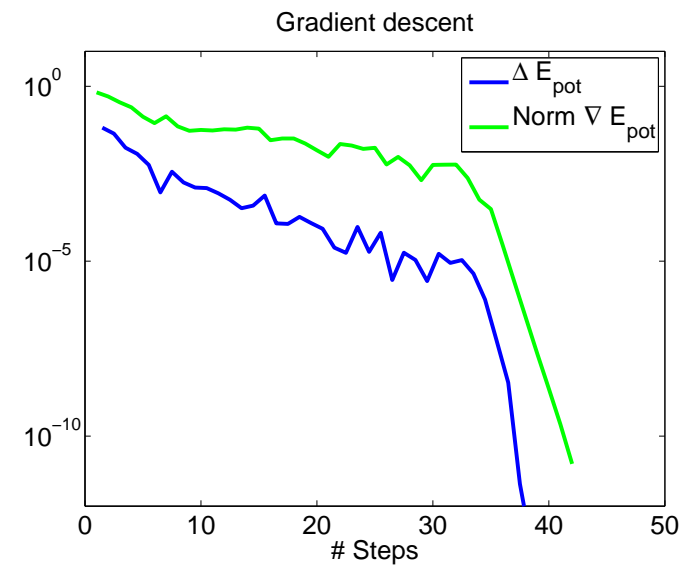
- ▶  $\vec{p}^t A \vec{p} < 0$ , return  $\vec{s}_* = \vec{s} + \alpha_b \vec{p}$ , such that  $\|\vec{s} + \alpha_b \vec{p}\| = \Delta$
- ▶  $\|\vec{s} + \alpha \vec{p}\| > \Delta$ , return  $\vec{s}_* = \vec{s} + \alpha_b \vec{p}$ , such that  $\|\vec{s} + \alpha_b \vec{p}\| = \Delta$
- ▶  $\|\vec{r}\| < \epsilon \|\vec{b}\|$ , return  $\vec{s}_* = \vec{s}$



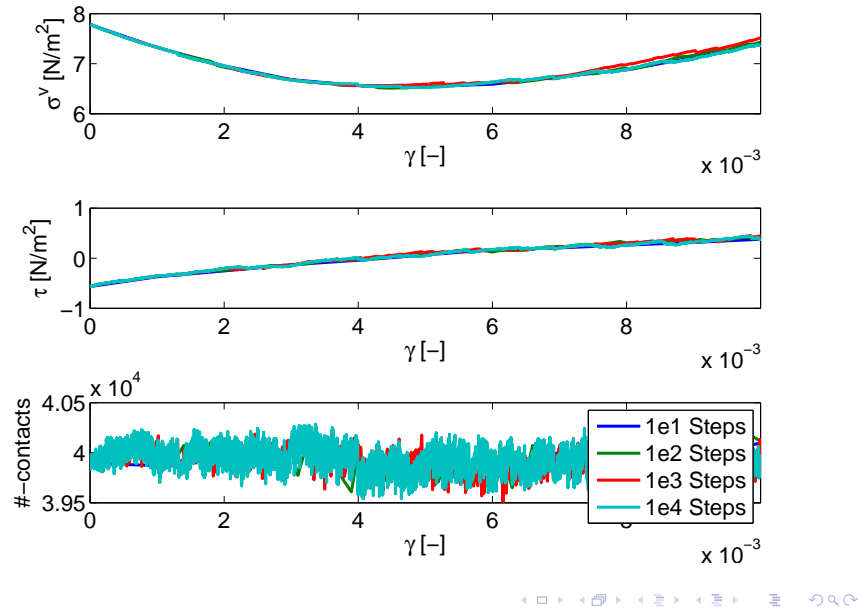
## Trust region video



## Trust region convergence



## Energy minimisation stresses



## Computational time

Number of time steps	Computational time
$10^1$	89 min $\approx$ 1.5 hour
$10^2$	403 min $\approx$ 6.7 hour
$10^3$	1083 min $\approx$ 18 hour
$10^4$	3620 min $\approx$ 2.5 day

## Compare the two

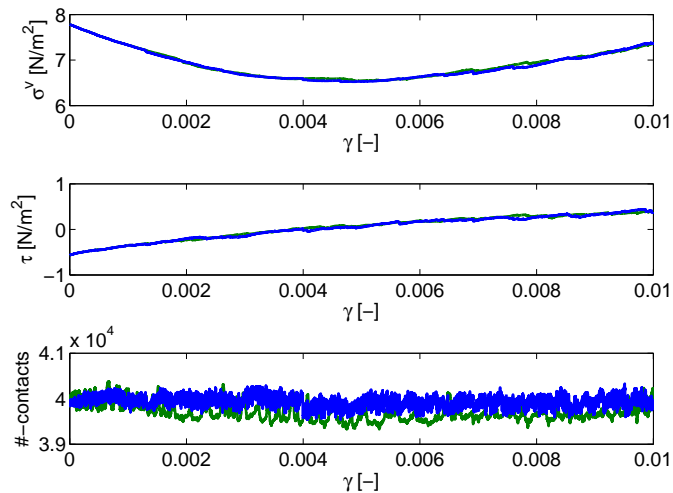


Figure: Blue = energy minimisation, red = discrete particle simulation

## Conclusion

- ▶ Energy minimisation and standard simulations give comparable output
- ▶ Required computational times are comparable
- ▶ Both processes can be optimised
- ▶ Not clear how the scaling of computational time on number of particles and packing fraction works